Various uses of statistical tools for texture analysis ICGIP-2016 *Tokyo October 30 2016*

Philippe Durand, Dariush Ghorbanzadeh and Luan Jaupi
Conservatoire national des arts et métiers Paris

25 octobre 2016

Presentation

Presentation

Presentation

Presentation

1. Introduction
2. Geostatistical texture
3. Texture interpolation
4. Granulometric extraction

Presentation

1. Introduction
2. Geostatistical texture
3. Texture interpolation
4. Granulometric extraction
5. Conclusions

Introduction

Abstract

The tools developed by **the School of geostatistic** have many applications for image segmentation . First, it is very suited to the analysis of natural images eg from **remote sensing images** and medical images. secondly, they are **less expensive** in time calculation, as can the methods, from Fourier analysis or matrices coocurrences. We offer reviews of **various works** of authors to **segment natural textures**.

Introduction

Abstract

The tools developed by **the School of geostatistic** have many applications for image segmentation . First, it is very suited to the analysis of natural images eg from **remote sensing images** and medical images. secondly, they are **less expensive** in time calculation, as can the methods, from Fourier analysis or matrices coocurrences. We offer reviews of **various works** of authors to **segment natural textures**.

Keywords

Fractal, Geostatistic, Variogram, granulometry.

Introduction

Introduction

Analysis of texture, realistic natural scenes interpolation requires **specific tools**. the geostatistical tools combines **geological approach**, structural approaches, and **statistical analysis**. In First part we describe a **very useful geostatistical tools** : **the variogram**. This tool generalizes the autocorrelation function. We give applications to separate natural textures in remote sensing. Another application that we describe is **the texture interpolation**. In the second part, we show how **the particle size analysis**, and the use of structural elements, allows the separation of textures on noisy images from SAR scenes.

Geostatistical texture

Mathematical morphology

The statistical approach that has historically proposed by Haralick (coocurences matrices) is the best because it contains lots of information. Unfortunately it costs much computation time. The geostatistical approach from ***mathematical morphology*** is very convenient.

Geostatistical texture

Mathematical morphology

The statistical approach that has historically proposed by Haralick (coocurences matrices) is the best because it contains lots of information. Unfortunately it costs much computation time. The geostatistical approach from ***mathematical morphology*** is very convenient.

Variogram

In the geostatistical approach, a tool well suited to the analysis of texture is the variogram. It can characterize different textures : periodicals (dune fields), fractals (***fractional Brownian motion***) (Clouds) ;

Geostatistical texture

Mathematical morphology

The statistical approach that has historically proposed by Haralick (coocurences matrices) is the best because it contains lots of information. Unfortunately it costs much computation time. The geostatistical approach from ***mathematical morphology*** is very convenient.

Variogram

In the geostatistical approach, a tool well suited to the analysis of texture is the variogram. It can characterize different textures : periodicals (dune fields), fractals (***fractional Brownian motion***) (Clouds) ;

Flexibility of the concept

The concept of variogram adapts to different situations we recall the main ***fractals*** and fractional Brownian motion, exponential variograms : well suited for periodic textures.

Fractal, fractional brownian motion

White noise is defined by :
$\langle W(t), W(t') \rangle = \sigma^2 \delta(t - t')$

Fractal, fractional brownian motion

White noise is defined by :
$\langle W(t), W(t') \rangle = \sigma^2 \delta(t - t')$
Brownian motion can be seen as an ***integration*** :

Fractal, fractional brownian motion

White noise is defined by :
$\langle W(t), W(t') \rangle = \sigma^2 \delta(t - t')$
Brownian motion can be seen as an ***integration*** :
$B(t) - B(0) = \int_{-\infty}^{t} W(t')dt'$

Fractal, fractional brownian motion

White noise is defined by :

$\langle W(t), W(t') \rangle = \sigma^2 \delta(t - t')$

Brownian motion can be seen as an ***integration*** :

$$B(t) - B(0) = \int_{-\infty}^{t} W(t')dt'$$

Fractional Brownian Motion

Mandelbrot and Ness (1968) suggest the following generalization (1) :

$$\Delta B_H(t) = B_H(t) - B_H(0) = \frac{1}{\Gamma(H + 1/2)} \int_{-\infty}^{t} K(t - t')W(t')dt' \text{ with}$$

$$K(t - t') = \begin{cases} (t - t')^{H-1/2}, & 0 \leq t' \leq t\,; \\ (t - t')^{H-1/2} - (-t')^{H-1/2}, & t' \leq 0. \end{cases}$$

Fractal, fractional brownian motion

White noise is defined by :
$\langle W(t), W(t')\rangle = \sigma^2\delta(t-t')$
Brownian motion can be seen as an ***integration*** :
$B(t) - B(0) = \int_{-\infty}^{t} W(t')dt'$

Fractional Brownian Motion

Mandelbrot and Ness (1968) suggest the following generalization (1) :
$\Delta B_H(t) = B_H(t) - B_H(0) = \frac{1}{\Gamma(H+1/2)}\int_{-\infty}^{t} K(t-t')W(t')dt'$ with
$K(t-t') = \begin{cases} (t-t')^{H-1/2}, & 0 \leq t' \leq t\,; \\ (t-t')^{H-1/2} - (-t')^{H-1/2}, & t' \leq 0. \end{cases}$

Remarks

(1) : When $H = 1/2$, we find the classical Brownian motion
(2) : $\Delta B_H(\lambda t) = \lambda^H \Delta B_H(t)$ if $t = 1$, $\Delta B_H(\lambda) = \lambda^H \Delta B_H(1)$:
autosimilarity $\Rightarrow$Fractal model

Example of de Fractional Brownian Motion

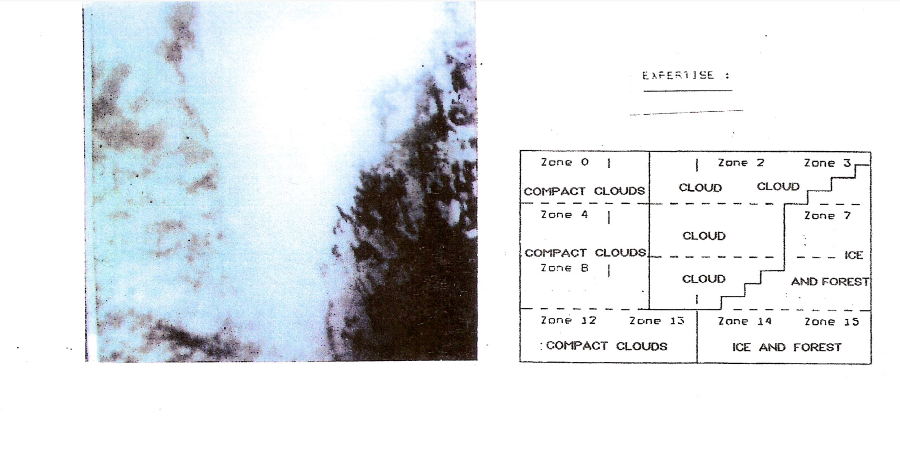

FIGURE:

Texture cloud

Variogram and FBM

Variogram

We consider a **homogeneous**$^{(*)}$ texture bath, the **variogram** is given by :
$2\gamma(h) = E[(f(x) - f(x+h))^2] = var(f(x) - f(x+h))$
If we denote C the covariance ($C(h) = E(f(x)f(x+h))$ thus :
$E[(f(x) - f(x+h))^2] = E(f(x)^2) - 2E(f(x)f(x+h)) + E(f(x+h)^2)$
With $(*)$: $2\gamma(h) = 2E(f(x))^2 - 2E(f(x)f(x+h)) = 2(C(0) - C(h))$

Variogram and FBM

Variogram

We consider a **homogeneous**$^{(*)}$ texture bath, the **variogram** is given by :
$2\gamma(h) = E[(f(x) - f(x+h))^2] = var(f(x) - f(x+h))$
If we denote C the covariance ($C(h) = E(f(x)f(x+h))$ thus :
$E[(f(x) - f(x+h))^2] = E(f(x)^2) - 2E(f(x)f(x+h)) + E(f(x+h)^2)$
With $(*)$: $2\gamma(h) = 2E(f(x))^2 - 2E(f(x)f(x+h)) = 2(C(0) - C(h))$

Fractional Brownian Motion

For an signal we adapt (1) :

$$\Delta B_H(x,t) = B_H(x+t) - B_H(x) = \frac{1}{\Gamma(H+1/2)} \int_{-\infty}^{t} K(t-t')W(t')dt'$$

and from the previous remark :
$var(\Delta B_H(x,\lambda)) = \lambda^{2H} var(\Delta B_H(x,1))$, we set $\sigma^2 = var(\Delta B_H(x,1))$

Variogram and FBM

Variogram

We consider a **homogeneous**$^{(*)}$ texture bath, the **variogram** is given by :
$2\gamma(h) = E[(f(x) - f(x+h))^2] = var(f(x) - f(x+h))$
If we denote C the covariance $(C(h) = E(f(x)f(x+h))$ thus :
$E[(f(x) - f(x+h))^2] = E(f(x)^2) - 2E(f(x)f(x+h)) + E(f(x+h)^2)$
With $(*)$: $2\gamma(h) = 2E(f(x))^2 - 2E(f(x)f(x+h)) = 2(C(0) - C(h))$

Fractional Brownian Motion

For an signal we adapt (1) :

$$\Delta B_H(x,t) = B_H(x+t) - B_H(x) = \frac{1}{\Gamma(H+1/2)} \int_{-\infty}^{t} K(t-t')W(t')dt'$$

and from the previous remark :
$var(\Delta B_H(x,\lambda)) = \lambda^{2H} var(\Delta B_H(x,1))$, we set $\sigma^2 = var(\Delta B_H(x,1))$

Fractal variogram

Thus from previous item, fractal variogram is given by $2\gamma_f(h) = h^{2H}\sigma^2$, with $D = d + 1 - H$ the ***fractal dimension***

Other variogram

Exponential Variogram

A variogram model specially adapted to periodic textures is ***exponential model*** given by :
$2\gamma_e(h) = C(1 - exp(-h/a))$ in this,
$C = E(f(x)f(x))$: ***covariance*** , a : measure ***correlation support***.

Other variogram

Exponential Variogram

A variogram model specially adapted to periodic textures is ***exponential model*** given by :

$2\gamma_e(h) = C(1 - exp(-h/a))$ in this,

$C = E(f(x)f(x))$: ***covariance*** , a : measure ***correlation support***.

Linear

Theorical ***linear*** variogram is given by

$2\gamma_l(h) = ph + q$

p : ***slope***, q : ***y-intercept***

Other variogram

Exponential Variogram

A variogram model specially adapted to periodic textures is ***exponential model*** given by :
$2\gamma_e(h) = C(1 - exp(-h/a))$ in this,
$C = E(f(x)f(x))$: ***covariance*** , a : measure ***correlation support***.

Linear

Theorical ***linear*** variogram is given by
$2\gamma_l(h) = ph + q$
p : ***slope***, q : ***y-intercept***

First step

Determine ***locally*** the six parameters of textures of these models from experimental variograms and the ***distance*** between experimental variogam and the three models ; thus realize vector of size nine : ***local signature*** of texture.

Experimental tools

Experimental Variogram

Let ***U neighborhood analysis***, For $(x+h, y+h) \in U$ We compute the quantity :

$Df_{x,y}((x,y),h) = \frac{1}{2}[(f(x+h,y) - f(x,y))^2 + (f(x,y+h) - f(x,y))^2]$

Experimental variogram is given by :

$$2\gamma(U,h) = \frac{1}{n(h)} \sum_{(x+h,y+h)\in U} Df_{xy}((x,y),h) \text{ with}$$

$n(h)$ is the number of pixels where both (x,y), $(x+h,y+h)$ ∈U

Experimental tools

Experimental Variogram

Let ***U neighborhood analysis***, For $(x+h, y+h) \in U$ We compute the quantity :

$Df_{x,y}((x,y),h) = \frac{1}{2}[(f(x+h,y) - f(x,y))^2 + (f(x,y+h) - f(x,y))^2]$

Experimental variogram is given by :

$$2\gamma(U,h) = \frac{1}{n(h)} \sum_{(x+h,y+h)\in U} Df_{xy}((x,y),h) \text{ with}$$

$n(h)$ is the number of pixels where both (x,y), $(x+h, y+h) \in$U

Fractal parameter

With linear regression on logarithmic variogram :

$ln(2\gamma(U,h)) = 2hH(U)ln(h) + 2ln(\sigma(U))$

-$d = 3 - H(U)$ is ***local*** fractal dimension

-$\sigma(U)$ is ***local*** standard deviation

Experimental tools

Experimental Variogram

Let ***U neighborhood analysis***, For $(x+h, y+h) \in U$ We compute the quantity :

$Df_{x,y}((x,y),h) = \frac{1}{2}[(f(x+h,y) - f(x,y))^2 + (f(x,y+h) - f(x,y))^2]$

Experimental variogram is given by :

$$2\gamma(U,h) = \frac{1}{n(h)} \sum_{(x+h,y+h)\in U} Df_{xy}((x,y),h) \text{ with}$$

$n(h)$ is the number of pixels where both (x,y), $(x+h, y+h) \in$U

Fractal parameter

With linear regression on logarithmic variogram :

$ln(2\gamma(U,h)) = 2hH(U)ln(h) + 2ln(\sigma(U))$

-$d = 3 - H(U)$ is ***local*** fractal dimension

-$\sigma(U)$ is ***local*** standard deviation

Linear parameter

With linear regression on variogram : $2\gamma(U,h) = p(U)h + q(U)$

$p(U)$ is ***local*** slope , $q(U)$ is ***local*** y-intercept

Local texture parameters

Fractal parameter

With linear regression on logarithmic variogram :
$ln(2\gamma(U,h)) = 2hH(U)ln(h) + 2ln(\sigma(U))$

-$d = 3 - H(U)$ is ***local*** fractal dimension
-$\sigma(U)$ is ***local*** standard deviation

Local texture parameters

Fractal parameter

With linear regression on logarithmic variogram :
$ln(2\gamma(U,h)) = 2hH(U)ln(h) + 2ln(\sigma(U))$

-$d = 3 - H(U)$ is ***local*** fractal dimension
-$\sigma(U)$ is ***local*** standard deviation

Linear parameter

With linear regression on variogram : $2\gamma(U,h) = p(U)h + q(U)$

-$p(U)$ is ***local*** slope
-$q(U)$ is ***local*** y-intercept

Local texture parameters

Fractal parameter

With linear regression on logarithmic variogram :
$ln(2\gamma(U,h)) = 2hH(U)ln(h) + 2ln(\sigma(U))$

-$d = 3 - H(U)$ is ***local*** fractal dimension
-$\sigma(U)$ is ***local*** standard deviation

Linear parameter

With linear regression on variogram : $2\gamma(U,h) = p(U)h + q(U)$

-$p(U)$ is ***local*** slope
-$q(U)$ is ***local*** y-intercept

Exponential parameter

$2\gamma(h) = C(U)(1 - exp(-h/a(U)))$

-$a(U)$ is ***local*** slope at the origin
-$C(U)$ is ***local*** coovariance.

Challenge, separating sea ice and clouds

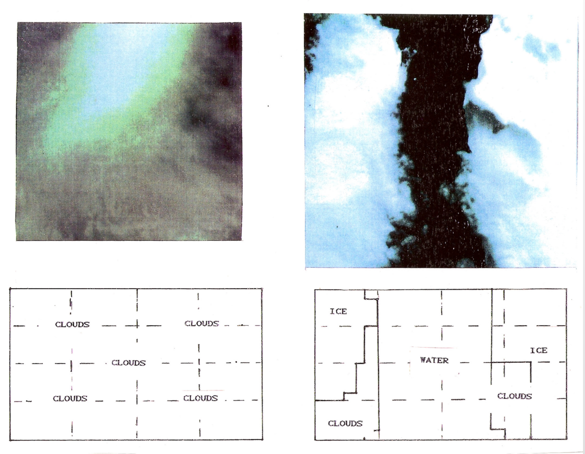

FIGURE:

Texture cloud

Local signature

Distance to models

We calculate a ***distance*** for each windows between experimental variogram and model (fractal, exponential or linear) :

$D_{mod}(U)) = \Sigma_h |\gamma(U,h) - \gamma_{mod}(U,h)|^2$

Local signature

Distance to models

We calculate a ***distance*** for each windows between experimental variogram and model (fractal, exponential or linear) :

$D_{mod}(U)) = \Sigma_h|\gamma(U,h) - \gamma_{mod}(U,h)|^2$

Parameter vector

for each window we compute :

$V(U) = (H(U), \sigma(U), a(U), C(U), p(U), q(U), D_f(U), D_e(U), D_l(U))$

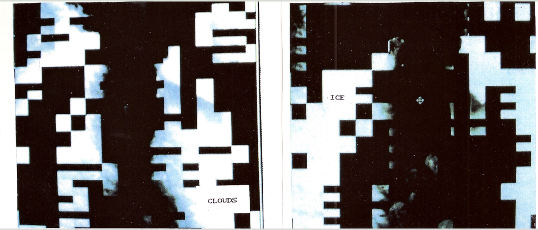

FIGURE: Nearest model : left fractal, right linear

Texture interpolation

Fractal interpolation

Another problematic involving the statistical analysis of the texture is **texture interpolation**. Interpolation methods are commonly used : the **bicubic interpolation** or smoothing methods such as spines. these methods are not desirable when you want to **preserve the appearance of a texture**. we can take the approach of interpolation by the technique of the **midpoint proposed by Mandelbrot**. This technique can be improved by an interpolation directly involving **local variogramme at a point**.

Texture interpolation

Fractal interpolation

Another problematic involving the statistical analysis of the texture is **texture interpolation**. Interpolation methods are commonly used : the **bicubic interpolation** or smoothing methods such as spines. these methods are not desirable when you want to **preserve the appearance of a texture**. we can take the approach of interpolation by the technique of the **midpoint proposed by Mandelbrot**. This technique can be improved by an interpolation directly involving **local variogramme at a point**.

Kriging interpolation

Another method **directly involving the notion of variogram** is the **notion of kriging**.We distinguish the **simple kriging**, the resampled image is considered as an intrinsic random variable $Z(x)$. Given the ergodicity criterion, the method involves estimating the central point $Z(x_0)$ knowing the variogram $\Gamma(h)$, stationary near the x_0 point and a **polygon** defined by the n points : $x_2, ...x_n$ surrounding x_0.

Texture interpolation

Kriging interpolation

$$E(Z'(x) - Z(x_0)) = 0 \tag{1}$$

with, $E((Z'(x) - Z(x_0))^2) = \sigma^2(x_0)$ mininum
We choice $Z'(x_0)$ as linear combination :

$$Z'(x_0) = \sum_{i=1}^{n} \lambda_i Z(x_i) \tag{2}$$

The prroblem is to determine λ_i, this leads to the optimization method :

$$\begin{gathered} \sum_{i=1}^{n} \lambda_i \Gamma_{ij} + \mu = \Gamma_{i0} \\ \sum_{i=1}^{n} \lambda_i = 1 \end{gathered} \tag{3}$$

μ is Lagrange parameter, Γ_{ij} the semivariance between x_i and x_j, Γ_{i0} the semivariance between x_i and interpolate point x_0

Comparaison between interpolates methods

Co-kriging

We can also consider the **co-kriging is an interpolation technique** to observe the stochastic behavior of multivariate spatial data. as for the simple kriegeage, we try to interpolate the function $Z(x)$, but there is more to the data of **other channels** $Z_l(x)$. In these methods, the choice of a variogram modeled from fractal analysis gives the best results for interpolation of natural reliefs.

Comparaison between interpolates methods

Co-kriging

We can also consider the **co-kriging is an interpolation technique** to observe the stochastic behavior of multivariate spatial data. as for the simple kriegeage, we try to interpolate the function $Z(x)$, but there is more to the data of **other channels** $Z_l(x)$. In these methods, the choice of a variogram modeled from fractal analysis gives the best results for interpolation of natural reliefs.

Comparisons

We have for the region of Beni Chougrane (Algeria), a SPOT **panchromatic data**, and a data SPOT XS2. Is obtained, after these different treatments, a fractal interpolation image, a kriged image, a co-kriged image, using the covariogram, that is to say a cross variogram between data of the same scene but from the image panchromatic. We compare **the first two moments** (mean and standard deviation). the following table is obtained :

Comparaison between interpolates methods

Results

	Panchromatic	XS2	Fractal	Krige	Co-krige
Mean	84,3	70,6	71,9	70,3	84,9
Standard deviation	54,2	49,4	47,5	49,4	54,9

Comparaison between interpolates methods

Results

	Panchromatic	XS2	Fractal	Krige	Co-krige
Mean	84,3	70,6	71,9	70,3	84,9
Standard deviation	54,2	49,4	47,5	49,4	54,9

Comparaison between interpolates methods

Results

	Panchromatic	XS2	Fractal	Krige	Co-krige
Mean	84,3	70,6	71,9	70,3	84,9
Standard deviation	54,2	49,4	47,5	49,4	54,9

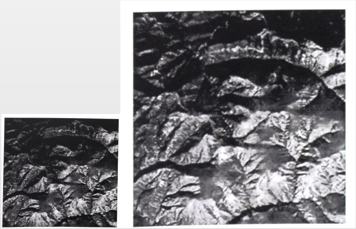

FIGURE: : Interpolation by kriging of Spot Panchromatique in Algeria

Comparaison between interpolates methods

Results

	Panchromatic	XS2	Fractal	Krige	Co-krige
Mean	84,3	70,6	71,9	70,3	84,9
Standard deviation	54,2	49,4	47,5	49,4	54,9

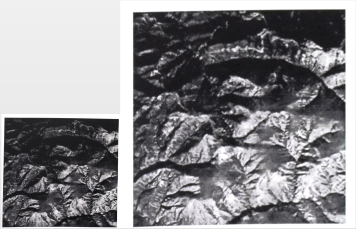

FIGURE: : Interpolation by kriging of Spot Panchromatique in Algeria

The results are substantially identical, the mean and standard deviation are preserved compared with the initial datas. Figure 2 visually attest to the similarity between the image and its interpolation

Interpolation by Kriging

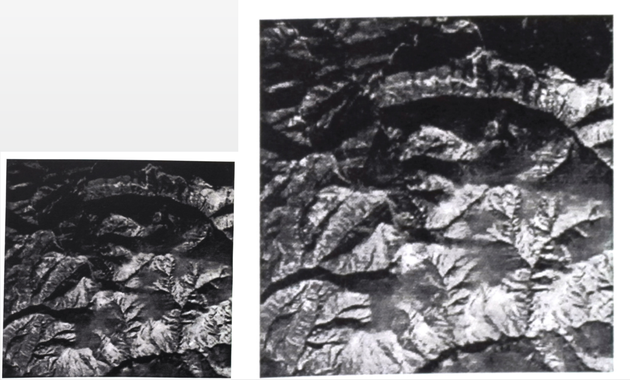

FIGURE: : Interpolation by kriging of Spot Panchromatique in Algeria

Morphological processing of noisy radar images

Radar Images

Radar images particles in SAR images are noisy by the **speckle noise**. eliminating the noise by smoothing methods lose much of the radar information. another alternative to solve this problem is to consider that noise is a source of information. the use of **topological methods** to extract and classify particle sizes can **bring interesting results**

Morphological processing of noisy radar images

Radar Images

Radar images particles in SAR images are noisy by the **speckle noise**. eliminating the noise by smoothing methods lose much of the radar information. another alternative to solve this problem is to consider that noise is a source of information. the use of **topological methods** to extract and classify particle sizes can **bring interesting results**

Urban network extraction

We have an SAR image of an urban area of southern France.This scene includes an urban area comprising its roadworks, a **large urban cores**, and a set of **HLM**. The raw image is very noisy and it is difficult to distinguish the pixels belonging to the urban network, those noise. A particle size sieving, thanks to a composition of opening closing, increasing in size, give the colored composition of Figure 3. that helps to distinguish from road network, **suburban housing**, set of HLM and a large urban core.

Morphological processing of noisy radar images

FIGURE: : Sar Image of Le-Luc Town and particle extraction of the urban network

Morphological processing of noisy radar images

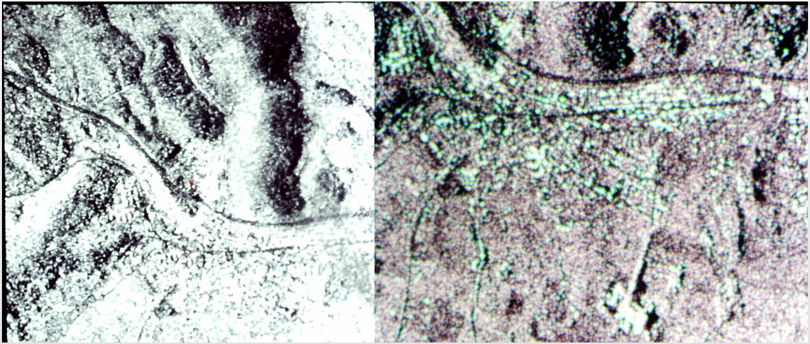

FIGURE: : Sar Image of Le-Luc Town and particle extraction of the urban network

Morphological processing of noisy radar images

Comment of this method

the figure represents a **composition of morphological openings** : a composition of erosion-dilatation. The **erosion** component, **sculpting, relief**, and highlights the roadworks while the **dilatation** component **strengthens the built**. An image is obtained where the different textural components are well cleared. In conclusion we can say that the dilatation reinforces the strong radiometric and makes more uniform texture, erosion enhances contrasts relief. These manipulations are intended to show the interest of mathematical morphology. It represents a **first step in the organization** of a scene data in order to address texture analysis.

Morphological processing of noisy radar images

Comment of this method

the figure represents a **composition of morphological openings** : a composition of erosion-dilatation. The **erosion** component, **sculpting, relief**, and highlights the roadworks while the **dilatation** component **strengthens the built**. An image is obtained where the different textural components are well cleared. In conclusion we can say that the dilatation reinforces the strong radiometric and makes more uniform texture, erosion enhances contrasts relief. These manipulations are intended to show the interest of mathematical morphology. It represents a **first step in the organization** of a scene data in order to address texture analysis.

Comparaison with other methods

One of the main method of texture analysis is the **coocurence matrices** method. we extracted characteristic target areas on the image for example in the suburban housing. when, after calculating coocurences matrices, we are interested in **index homogeneity** is observed that the housing is restored. However, this method does **nothing more visually** than mathematical morphology, and **the calculations are more delicate**.

conclusion

conclusion

These few applications, demonstrated the **interest of the application of morphological methods** for remote sensing images. the **variogram is well adapted to the modeling of natural textures**. moreover its inclusion in the interpolation allows realistic enlargements. Using operators segmenting the **particle size is particularly well suited to the study of radar images**. unlike the smoothing, it can not eliminate valuable information hidden in the noise.

VII) Références

- Brunet G. ,Durand Ph., J Devars *System for automatic knowledge-based detection of Clouds in aerial images*, Artificial intelligence applications and neurals networks, Zurich Juin 25-27 1990.
- Brunet G. P Durand, Rudant JP. *A knowledge-based system for interpretation of satellite pictures* IEEE International Geoscience And Remote Sensing Symposium and Helsinki (IGARSS), Finland, June 3-6 1991
- Ph. Durand, Hakdaoui, J Chorowicz, J.P Rudant, A. Simonin *Caracterisation des textures urbaines sur image radar Varan par approche morphologique et statistique. Application a la ville du Luc (sud-est de la France)* Int. J. Remote sensing, 1994, vol 15, no 5, 1065-1078
- Mandelbrot B.B. and Ness J.V. (1968) *Fractional Brownian motions, fractional noise and applications* SIAM review 10, pp. 422-437
- Mathéron G (1967) *Eléments pour une théorie des milieux poreux* Masson éd.

- Pentland A. (1984) *Fractal-based description of natural scènes IEEE* Trans. Pattern anal. Machine Intell. 6, 661, 674
- Ramstein G. Raffy M. (1986) *Caractérisation multispectrale de la structure spatiale des images de télédetection*, Signatures spectrale d'objets en télédetection, quatrième Colloque Intern. Janv 1988, Aussois.
- Ramstein G. Raffy M. (1989) *Analysis of the structure of radiometric remotely -sensed images* , Intern. J. of remote Sensing vol. 10 n°6 pp. 1049, 1073